AIAA JOURNAL
Vol. 32, No. 6, June 1994

Governing Equations and Finite Element Models for Multiaxial Piezoelectric Beam Sensors/Actuators

Rong C. Shieh*
MRJ, Inc., Oakton, Virginia 22124

Governing equations and finite element models for multiaxially active laminated piezoelectric beam sensor/actuator elements capable of simultaneously sensing/actuating all four components (axial extension, biaxial bendings, and torsional twisting) of beam deformation are presented and used in special sensor/actuator pair designs as well as finite element analysis for transient responses of adaptive frame structures partially composed of these active beam elements.

I. Introduction

In a recent study[1] a three-dimensional laminated piezoelectric beam sensor/actuator theoretical model has been advanced and applied in the design of multiaxially active piezoelectric sensor/actuator beam elements by use of the "four-sectored" type design concept. The present study is the second part (finite element formulation) of a two-part study of a beam sensor/actuator design/analysis technology development program. The study program represents a major extension of the current state-of-the-art technology in this area, which is currently limited primarily to the uniaxial extensional and/or bending deformation cases. The general theory and/or design are based on the elementary beam assumptions (with proper adjustment to include the cross-sectional warping effect) and incorporate the advanced design concepts of piezoelectric laminate (i.e., varying lamina skew angle, reshaping the surface electrode pattern, varying the polarization profile, and laminating different piezoelectric laminae) in the developments. Most of the previous laminated piezoelectric beam sensor/actuator studies[3-9] are based on the conditions of uniform surface electrode pattern, constant polarization profile, and zero lamina skew angle, although all of these four design parameters are considered[8,9] for design of laminated piezopolymer platesensors/actuators.

To completely and simultaneously control all (four) deformation components of a beam element, a new concept has been developed by deploying four sets of single or multiple laminated (layered) actuator/sensor pairs that are symmetrically bonded to the four-sectored, outer surface(s) of the biaxially symmetric cross-section structural core.[1] This active piezoelectric beam design concept is exemplified by the circular and rectangular cross-section cases in which each of four sets of polyvinylidene fluoride polymer (PVF_2 or PVDF) piezoelectric sensor/actuator pairs (laminae) are bonded to each of the four outer surfaces of the hollow (or solid) structure core, designated as "four-sectored sensor/actuator pair" design. (Most of the previous rod or beam sensor/actuator studies deal with the solid cross-section case, whereas actual space structures mostly have rectangular or circular tubular beam cross sections, as considered in the present study.)

In the present study, the governing equations for laminated piezoelectric beams and four-sectored beam sensors/actuators derived elsewhere[1] are summarized and extended to the Kelvin-Voigt viscoelastic material case in Sec. II. The corresponding variational actuator equations of motion are formulated in Sec. III. The latter and sensor equations are then used in developing the finite active piezoelectric beam sensor/actuator element model that follows the negative strain rate feedback control law in Sec. IV. Two special active finite beam element models under the uniformly distributed surface electrode/polarization profile case are then developed for the hollow (or solid) rectangular beam cross-section case in Sec. V. One of the special active beam elements is used in an example space antenna frame in Sec. VI to demonstrate their effectiveness in three-dimensional multiaxial vibration control of flexible space structures via study of transient structural response behavior as a function of control gain parameter.

II. Extension of Previous Work to Viscoelastic Material Case

Consider a composite beam element of length L comprised of a hollow (or solid) elastic host structure and longitudinally continuous laminated piezoelectric strips of PVDF (or PVF_2) and/or lead-ziconate-titanate (PZT) piezoceramic type that are biaxially symmetrically bonded to the outer surfaces of the biaxially symmetric cross-sectional structure core. The beam element is assumed to undergo three-dimensional motion. Let x'(or 1′) and y' (or 2′) be the two principal material axes normal to the poling (thickness) direction, i.e., the z' (or 3′) axis direction as shown in Fig. 1. Also shown in Fig. 1 are the beam (x, y, z) and intermediate (x'', y'', z'') Cartesian coordinate systems for a rectangular cross-section beam element case. In the beam coordinate system, x (or 1) is the beam centroidal axis, and y (or 2) and z (or 3) are the two principal axes of a biaxially symmetric beam cross section. The intermediate coordinate system (x'', y'', z'') is introduced here to facilitate the coordinate transformations between the beam

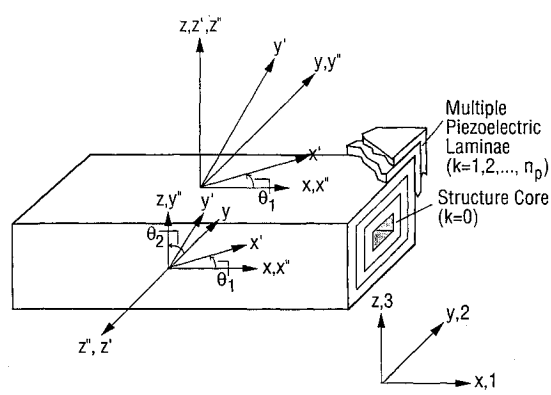

Fig. 1 Material, beam, and intermediate coordinate systems (x', y', z'), (x, y, z), and (x'', y'', z'').

Received Feb. 15, 1993; presented as Paper 93-1687 at the AIAA/ASME/ASCE/AHS/ASC 34th Structures, Structural Dynamics, and Materials Conference, La Jolla, CA, April 19-21, 1993; revision received Oct. 13, 1993; accepted for publication Oct. 13, 1993.

*Member of Technical Staff, Aerospace Division, 10455 White Granite Drive. Member AIAA.

coordinate system (x, y, z) and the lamina coordinate system (x', y', z'). The $x''y''z''$ coordinate frame is obtained by rotating the xyz coordinate frame counterclockwise by an orientation angle θ_2 with respect to the x axis so that the z'' axis is normal to the surface element of interest. The $x'y'z'$ coordinate frame is obtained by rotating the $x''y''z''$ coordinate frame counterclockwise by an angle (designated as "skew angle") θ_1, with respect to the z'' axis so that x', y', and z' axes coincide with the lamina principal axes.

Under the Euler-Bernoulli elementary beam assumptions and by incorporating four key design parameters of piezoelectric laminate design, the actuator equations of motion and sensor equations have been derived earlier[1] for general laminated piezoelectric beams of biaxially symmetric cross-section type. To take into account general cross-sectional warping (except for the circular cross-section case) due to torsional deformation, replacement of the polar moment of inertia I_0 with the torsional constant J in the torsional equation of motion, derived under the Euler-Bernoulli assumptions, has been made.[1] The secondary effects, such as the shear deformation, rotatory inertia, and secondary warping effects,[14,15] have been neglected in the derivations. The mathematical model has been applied to design of multiaxial piezoelectric sensor/actuator pair type based on the "four-sectored" design concept and negative strain rate feedback control law. For completeness and further development, these governing equations, with the present extension to the Kelvin-Voigt viscoelastic material case, are briefly presented next.

A. Governing Equations for Laminated Piezoelectric Beams

1. Extension of Governing Beam Equations to Kelvin-Voigt Viscoelastic Material Case

Consider the case in which host structural and piezoelectric lamina materials follow, respectively, the linear isotropic Kelvin-Voigt viscoelastic constitutive models[10] of the forms

$$\{\sigma\} = [C]\{\epsilon\} + [\eta]\{\dot{\epsilon}\} \tag{1a}$$

$$\{\sigma\} = [C]\{\epsilon\} + [\eta]\{\dot{\epsilon}\} - [C][d]\{E\} \tag{1b}$$

where $\{\sigma\}$ and $\{\epsilon\}$ are the (6×1) stress and strain vectors, respectively; $[C]$ and $[\eta]$ are the (6×6) elastic and viscous modulus matrices, respectively; $\{E\}$ is the (3×1) electric filed intensity vector; $[d]$ is the (6×3) piezoelectric strain constant matrix; and a dot indicates a time (t) derivative. The corresponding governing equations of motion for the laminated piezoviscoelastic beams made of such materials are obtained from their piezoelastic counterparts[1] by replacing the effective elastic composite beam extensional, biaxial bending, and torsional stiffnesses $(\overline{EA}, \overline{EI}_y, \overline{EI}_z, \overline{GJ})$ by the viscoeleastic differential operators, i.e.,

$$\{\overline{EA}, \overline{EI}_y, \overline{EI}_z, \overline{GJ}\} \rightarrow \{\overline{EA}, \overline{EI}_y, \overline{EI}_z, \overline{GJ}\} + \{\overline{\eta_E A}, \overline{\eta_E I_y}, \overline{\eta_E I_z}, \overline{\eta_G J}\}^T \partial/\partial t \tag{1c}$$

where $\eta_E A$, $\eta_E I_y$, $\eta_E I_z$, and $\eta_G J$ are the effective beam viscous stiffnesses. Thus, the governing beam (actuator) equations of motion are

$$(\overline{EA} + \overline{\eta_E A}\,\partial/\partial t)u''(x, t) - \overline{\rho A}\ddot{u}(x, t) = -N_p'(x, t) - p_u(x, t) \tag{2a}$$

$$(\overline{EI}_z + \overline{\eta_E I_z}\,\partial/\partial t)v''''(x, t) + \overline{\rho A}\ddot{v}(x, t) = M_{pz}''(x, t) + p_v(x, t) \tag{2b}$$

$$(\overline{EI}_y + \overline{\eta_E I_y}\,\partial/\partial t)w''''(x, t) + \overline{\rho A}\ddot{w}(x, t) = M_{py}''(x, t) + p_w(x, t) \tag{2c}$$

$$(\overline{GJ} + \overline{\eta_G J}\,\partial/\partial t)\beta''(x, t) - \overline{\rho I}_x\ddot{\beta}(x, t) = -M_{px}'(x, t) - p_\beta(x, t) \tag{2d}$$

where the piezoelectric stress resultants (axial force N_p; bending moments with respect to y and z axes, M_{py} and M_{pz}; and torsional moment M_{px}) are

$$N_p = -\sum_{k=1}^{n_p}\int_{A^k} E_{3'}^k(x', y', t)e_{31}^k(x', y')\,dA^k \tag{2e}$$

$$M_{py} = -\sum_{k=1}^{n_p}\int_{A^k} E_{3'}^k(x', y', t)e_{31}^k(x', y')z\,dA^k \tag{2f}$$

$$M_{pz} = -\sum_{k=1}^{n_p}\int_{A^k} E_{3'}^k(x', y', t)e_{31}^k(x', y')y\,dA^k \tag{2g}$$

$$M_{px} = -\sum_{k=1}^{n_p}\int_{A^k} E_{3'}^k(x', y', t)e_{36}^k(x', y')(n_2 y - m_2 z)\,dA^k \tag{2h}$$

In Eqs. (2a–2d), u, v, and w are the beam centroidal axis displacement components in the x, y, and z directions, respectively; $\overline{EA}$, $\overline{EI}_y$, $\overline{EI}_z$, and $\overline{GJ}$ are the effective axial (extensional), y-axis and z-axis bending, and torsional stiffnesses of the composite beam, respectively; $\overline{\rho A}$ and $\overline{\rho I}_x$ are the effective mass and torsional mass inertia per unit length of the composite beam, respectively; p_u, p_v, p_w, and p_β are the x, y, z, and torsional components of applied distributed forces/moment, respectively; a prime (with the exception of x', y', and z') indicates a derivative with respect to x. In Eqs. (2e–2h), A is the cross-sectional area; $(\,)^k$ the kth layer portion of cross section with $k = 0$ corresponding to the host structure core (or layer) portion of cross section; $E_{3'}^k$ is the electric field intensity component in the $3'$ (z') direction of the kth piezoelectric lamina; n_p is the number of piezoelectric laminae (layers); e_{3i} $(i = 1, 5, 6)$ (with superscripts $k = k$th lamina omitted for brevity) is the lamina piezoelectric stress constants in the z' $(3')$ direction given by

$$e_{31} = E(m_1^2 d_{3'1'} + n_1^2 d_{3'2'}) - 2Gm_1 n_1 d_{3'6'} \tag{2i}$$

$$e_{35} = e_{36} = G[2m_1 n_1(d_{3'1'} - d_{3'2'}) + (m_1^2 - n_1^2)d_{3'6'}] \tag{2j}$$

In Eqs. (2i) and (2j), E and G are the lamina material Young and shear moduli; $m_1 = \cos\theta_1$ and $n_1 = \sin\theta_1$ with θ_1 denoting the lamina skew angle (cf. Fig. 1); and $d_{3'i}$ $(i = 1', 2', 6')$ is the piezoelectric strain constants, which, under a variable polarization profile condition, can be expressed as

$$d_{3'i} = \bar{d}_{3'i}\xi_i(x', y')(i = 1', 2', 6') \tag{2k}$$

where ξ_i are the polarization profile functions.

The electric field $E_{3'}^k$ is related to the lamina voltage $V^k(t)$ in the thickness direction by

$$E_{3'}^k = V^k(t)\Psi^k(x', y')/t_{3'}^k \tag{3}$$

where $t_{3'}^k$ is the lamina thickness, and $\Psi^k(x', y')$ $(= 1$ or $0)$ is the effective surface electrode charge distribution function for the kth piezoelectric lamina.

2. Laminated Piezoelectric Beam Sensor Equations

Let q^k be the electric charge on the surface area of the kth piezoelectric lamina layer enclosed by $x = (0, L)$ and circumferential sector defined by circumferential coordinates $s^k = (s_1^k, s_2^k)$. Let $\Psi^k(x, s)$ be, as before, the effective surface electrode of the kth layer, i.e., $\Psi^k = 1$ or 0 according to whether the surface is covered by an effective surface electrode or not. With use of grounded closed-circuit design of the sensors, for which $E_{3'} = 0$ (Fig. 2), the sensor equation in electric current form is

$$i^k(t) = \frac{dq^k(t)}{dt} = \int_{s^{k1}}^{s^{k2}}\int_0^L \Psi^k(x, s)[e_{31}^k(\dot{u}' - y\dot{v}'' - z\dot{w}'') + (e_{35}^k n_2 y - e_{36}^k m_2 z)\dot{\beta}']\,dx\,ds \tag{4}$$

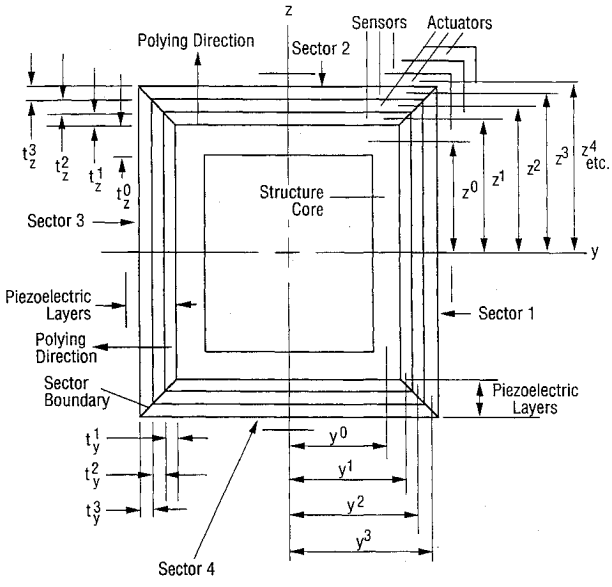

Fig. 2 Four-sectored, piezoelectrically laminated rectangular cross-section design.

where $ds = (dy^2 + dx^2)^{1/2}$ with s here denoting the beam cross-section circumferential coordinate, and $m_2 = \cos\Theta_2$, $n_2 = \sin\Theta_2$ with Θ_2, as before, denoting the surface orientation angle (cf. Fig. 1).

B. Four-Sectored Sensor/Actuator Pair Design of Negative Strain Rate Feedback Type

1. Four-Sectored Actuator/Sensor Design Concept

To efficiently control three-dimensional vibrations of a space frame structure, mixed use of the complete and partial deformation or deformation rate control concepts will be made. In the complete control, a total of four deformation components (extensional, biaxial bendings, and twisting) or their rate counterparts that are usually induced within each of the active beam elements (containing the multiaxial piezoelectric sensors/actuators) will be simultaneously controlled. To accomplish this, a new design concept of four-sectored design is introduced.[1] In this design concept, the biaxially symmetric beam cross section is artificially divided into four sectors that are geometrically symmetric with respect to the opposite sectors as well as the two principal cross-sectional axes (Fig. 3). The sector radial-longitudinal boundary surfaces are located at the four corners for the rectangular cross-section case and polar angles of, say, $\phi = \pm\phi_0$ and $\phi = 180 \text{ deg} \pm \phi_0$ for $0 < \phi_0 < 90$ deg for the circular cross-section case. To each of the four-sectored outer surfaces of the structure core at least one longitudinal strip of piezoelectric lamina layer is bonded symmetrically (with respect to the two principal cross-sectional axes) to serve as a sensor or actuator. The piezoelectric strip of each sector is assumed to extend to the full length of the beam element, but it may cover only the central strip or the entire width of the sector surface. If a feedback control that uses separate actuator and sensor units is of interest, at least a pair of piezoelectric sensor/actuator layers are required for each sector so that there are a total of four sets of single or multiple sensor/actuator pairs for an active laminated piezoelectric beam element.

Given next are the governing equations for the four-sectored laminated piezoelectric beam actuator/sensor design case of rectangular cross section under the equal polarization profile component condition [cf. Eq. (2k)]

$$\xi_{1'} = \xi_{2'} = \xi_{3'} \equiv \xi_{0'}(x', y') \tag{5}$$

The cases for circular cross section and/or general unequal polarization profile components have also been studied elsewhere by the author.[2]

2. Actuator Equations for Rectangular Cross-Section Case

In what follows, it is assumed that the odd and even number piezoelectric lamina layers, counting from the innermost layer outward, correspond to the sensor and actuator pair layers, respectively, so that there are a total of $n_{sa} = n_p/2$ pairs of sensor/actuator for each sector. The actuator equations of motion, Eqs. (2a–2d), specialized to the present design case satisfying Eq. (5) and in view of Eq. (3) now become

$$N_p(x, t) = -\sum_{k=2,4}^{n_p}\sum_{j=1}^{4} a^{k,j}\bar{e}_{31}^{k,j}V^{k,j} \tag{6a}$$

$$M_{py}(x, t) = -\sum_{k=2,4}^{n_p}\left[\sum_{j=1,3} b^{k,j}\bar{e}_{31}^{k,j}V^{k,j} + \sum_{j=2,4} z^k a^{k,j}\bar{e}_{31}^{k,j}V^{k,j}(-1)^{(j+2)/2}\right] \tag{6b}$$

$$M_{pz}(x, t) = -\sum_{k=2,4}^{n_p}\left[\sum_{j=2,4} b^{k,j}\bar{e}_{31}^{k,j}V^{k,j} + \sum_{j=1,3} y^k a^{k,j}\bar{e}_{31}^{k,j}V^{k,j}(-1)^{(j+3)/2}\right] \tag{6c}$$

$$M_{px}(x, t) = -\sum_{k=2,4}^{n_p}\left(y^k\sum_{j=1,3} a^{k,j}\bar{e}_{36}^{k,j}V^{k,j} + z^k\sum_{j=2,4} a^{k,j}\bar{e}_{36}^{k,j}V^{k,j}\right) \tag{6d}$$

in which, with the omission of superscripts k and j,

$$[e_{31}, e_{35}, e_{36}] = [\bar{e}_{31}, \bar{e}_{35}, \bar{e}_{36}]\xi_{0'} \tag{7a}$$

$$\bar{e}_{31}(\theta_1) = E(m_1^2\bar{d}_{3'1'} + n_1^2\bar{d}_{3'2'}) - 2Gm_1n_1\bar{d}_{3'6'} \tag{7b}$$

$$\bar{e}_{36}(\theta_1) = \bar{e}_{35} = G[2m_1n_1(\bar{d}_{3'1'} - \bar{d}_{3'2'}) + (m_1^2 - n_1^2)\bar{d}_{3'6'}] \tag{7c}$$

and

$$a^{k,j}(x) = \int_{-\alpha^k}^{\alpha^k}\Omega^{k,j}(x, \alpha)\,d\alpha \tag{8a}$$

$$b^{k,j}(x) = \int_{-\alpha^k}^{\alpha^k}\alpha\Omega^{k,j}(x, \alpha)\,d\alpha \tag{8b}$$

$$\Omega^{k,j}(x, \alpha) \equiv \xi_{0'}^{k,j}(x, \alpha)\Psi^{k,j}(x, \alpha) \tag{8c}$$

for $j = 1$–4; $k = 2, 4, \ldots, n_p$ (= even number); $\alpha = z$ if $j = 1, 3$; and $\alpha = y$ if $j = 2, 4$.

The corresponding strain rate sensor equation, Eq. (4), now becomes

$$i^{k,j}(t) = \int_0^L [a^{k,j}(\bar{e}_{31}^{k,j}\dot{u}' - \bar{e}_{36}^{k,j}z^k\dot{\beta}') - \bar{e}_{31}^{k,j}(b^{k,j}\dot{v}'' \pm a^{k,j}\dot{w}''z^k)]\,dx \tag{9a}$$

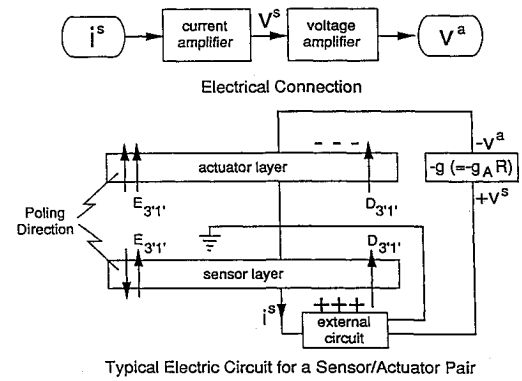

Fig. 3 Typical electric circuit loop for negative strain rate feedback sensor/actuator pair.

$$(j = 2, 4) \tag{9b}$$

$$i^{k,j}(t) = \int_0^L [a^{k,j}(\bar{e}_{31}^{k,j}\dot{u}' - \bar{e}_{36}^{k,j}y^k\dot{\beta}') - \bar{e}_{31}^{k,j}(b^{k,j}\dot{w}'' \pm a^{k,j}\dot{v}''y^k)]\,dx \tag{9c}$$

$$(j = 1, 3) \tag{9d}$$

for k = odd integer $(= 1, 3, \ldots, n_{p-1})$

3. Feedback Control Equations Via Piezoelectric Sensor/Actuator Pairs

Let the two successive $k = s_n = (2n-1)$th and $k = a_n = 2n$th $(n = 1, 2, \ldots, n_{sa} = n_p/2)$ piezoelectric layers be a typical nth conjugate sensor/actuator pair among a total of n_{sa} pairs in each of the four beam sectors. Because there is an interest in vibration jitter control through introduction of (active) piezoelectric damping to the system, a current amplifier for a piezoelectric sensor will be used. For such electric circuit arrangements, the sensor current, $i^{s_n,j}$, is related to the voltage $V^{s_n,j}$ by

$$V^{s_n,j} = R^{n,j}i^{s_n,j}(s_n = 2n-1;\ n = 1, \ldots, n_{sa};\ j = 1\text{–}4) \tag{10a}$$

or in a matrix form

$$\{V^s\}_n = [R]_n\{i^s\}_n \tag{10b}$$

where $R^{n,j}$ is the electric resistance at the jth sector of the nth sensor circuit at the jth sector.

The jth sector voltage output from a strain rate sensor is amplified by a factor $g_A^{n,j}$ and negatively fed back to its actuator counterpart of the conjugate, nth sensor/actuator pair, $V^{a_n,j}$, to counter the strain rates induced by external excitations (Fig. 2). Thus,

$$V^{a_n,j} = -g_A^{n,j}V^{s_n,j} = -g^{n,j}i^{s_n,j}(n = 1, \ldots, n_{sa};\ j = 1\text{–}4) \tag{11a}$$

or in a matrix form

$$\{V^a\}_n = -[g_A]_n\{V^s\}_n = -[g]_n\{i^s\}_n \tag{11b}$$

where

$$g^{n,j} = g_A^{n,j}R^{n,j} \tag{11c}$$

III. Variational Equations for Active Piezoelectric Beam Elements

Multiplication of variational virtual displacements, $-\delta v$, δv, $-\delta w$, and $-\delta\beta$, to Eqs. (2a–2d), respectively, addition of the resulting equations together, integration of the resulting equations with respect to x and t, and performance of partial integrations obtain

$$\int_0^t(\delta L - \delta W)\,dt = 0 \tag{12a}$$

where L is the Lagrangian and δW the external virtual work given by

$$L = \frac{1}{2}\int_0^L [\overline{EA}(u')^2 + \overline{EI_z}(v'')^2 + \overline{EI_y}(w'')^2 + \overline{GJ}(\beta')^2]\,dx - \frac{1}{2}\int_0^L [\overline{\rho A}(\dot{u}^2 + \dot{v}^2 + \dot{w}^2) + \overline{\rho I_x}\beta^2]\,dx \tag{12b}$$

$$\delta W = \int_0^t (N\delta u + Q_y\delta v + Q_z\delta w + M_x\delta\beta + M_y\delta\varphi_y + M_z\delta\varphi_z)_0^L\,dt - \int_0^t\int_0^L (\overline{\eta_E A}u'\delta u' + \overline{\eta_E I_z}v''\delta v'' + \overline{\eta_E I_y}w''\delta w'' + \overline{\eta_G J}\beta'\delta\beta')\,dx\,dt + \int_0^t\int_0^L (p_u\delta u + p_v\delta v + p_w\delta w + p_\beta\delta\beta)\,dx\,dt + \int_0^t\int_0^L (N_p\delta u' + M_{pz}\delta k_z + M_{py}\delta k_y + M_{px}\delta\beta')\,dx\,dt \tag{12c}$$

where

$$\varphi_y = -w', \quad \varphi_z = -v', \quad k_y = \varphi_y' = -w'', \quad k_z = \varphi_z' = -v'', \quad Q_y = M_z' = -\overline{EI_z}v''' + M_{pz}', \quad Q_z = M_y' = -\overline{EI_z}w''' + M_{py}' \tag{12d}$$

with Q_y and Q_z denoting the shear forces in the y and z directions, respectively.

The last term in the δW expression represents the virtual work done by the piezoelectric actuator forces/moments and can be regarded as the virtual internal work in the sensor signals feedback case. For the four-sectored design case, the piezoelectric stress resultants N_p, M_{py}, M_{pz}, and M_{px} are given by Eqs. (6a) and (6b), respectively.

IV. Finite Element Formulation of Active Piezoelectric Beam Elements

A. Interpolation Functions

Let subscripts A and B denote the quantities corresponding at the A and B ends of a beam element, and $\varphi_y = -w'$, $\varphi_z = v'$. By solving the unloaded static equations of equilibrium [Eqs. (2a–2d) with all terms except for the first ones dropped], the following are obtained as the interpolation functions for use in obtaining finite element models:

$$u = (1-\bar{x})u_A + \bar{x}u_B \qquad (\bar{x} = x/L) \tag{13a}$$

$$v = (1 + 2\bar{x}^3 - 3\bar{x}^2)v_A + (-2\bar{x}^3 + 3\bar{x}^2)v_B + L(\bar{x}^3 - 2\bar{x}^2 + \bar{x})\varphi_{zA} + L(\bar{x}^3 - \bar{x}^2)\varphi_{zB} \tag{13b}$$

$$w = (1 + 2\bar{x}^3 - 3\bar{x}^2)w_A + (-2\bar{x}^3 + 3\bar{x}^2)w_B - L(\bar{x}^3 - 2\bar{x}^2 + \bar{x})\varphi_{zA} - L(\bar{x}^3 - \bar{x}^2)\varphi_{zB} \tag{13c}$$

$$\beta = (1-\bar{x})\beta_A + \bar{x}\beta_B \tag{13d}$$

or in matrix form as

$$\{\mu\} = [\zeta(\bar{x})]\{U\} \tag{14a}$$

where $\varphi_{ij}(i = y, z;\ j = A, B)$ are positive counterclockwise and

$$\{\mu\} = \{u, v, w, \beta\}^T \tag{14b}$$

$$\{U\} = \{u_A, v_A, w_A, \beta_A, \varphi_{yA}, \varphi_{zA}, u_B, v_B, w_B, \varphi_{yB}, \varphi_{zB}, \beta_B\}^T \tag{14c}$$

B. Force-Displacement Relationships

Substituting Eqs. (13a–13d) and (6a–6d) into Eq. (12a) [with the aid of Eqs. (12b) and (12c)] and using the condition that variations $\{\delta U\}$ are arbitrary, there is obtained

$$\{F\}_e = [m]_e\{\ddot{U}\}_e + \{F_I\}_e - \{P\}_e \tag{15a}$$

where the (12×1) element end force vector $\{F\}_e$ is defined by

$$\{F\}_e = \{N_A, Q_{yA}, Q_{zB}, M_{xA}, M_{yA}, M_{zA}, N_B, Q_{yB}, Q_{zB}, M_{xB}, M_{yB}, M_{zB}\}_e^T \tag{15b}$$

which is associated with the end displacement vector $\{U\}_e$ and comes from the mechanical boundary force terms under the

$$[B^s] \Rightarrow [B^{s1}] = \begin{bmatrix} b_{11}^{s,1} & b_{12}^{s,1} & 0 & -b_{14}^{s,1} & 0 & b_{16}^{s,1} & -b_{11}^{s,1} & -b_{12}^{s,1} & 0 & b_{14}^{s,1} & 0 & b_{1,12}^{s,1} \\ b_{11}^{s,2} & 0 & b_{12}^{s,2} & -b_{14}^{s,2} & -b_{16}^{s,2} & 0 & -b_{11}^{s,2} & 0 & -b_{12}^{s,2} & b_{14}^{s,2} & -b_{1,12}^{s,2} & 0 \\ b_{11}^{s,3} & -b_{12}^{s,3} & 0 & -b_{14}^{s,3} & 0 & -b_{16}^{s,3} & -b_{11}^{s,3} & b_{12}^{s,3} & 0 & b_{14}^{s,3} & 0 & -b_{16}^{s,3} \\ b_{11}^{s,4} & 0 & -b_{12}^{s,4} & -b_{14}^{s,4} & b_{16}^{s,4} & 0 & -b_{11}^{s,4} & 0 & b_{12}^{s,4} & b_{14}^{s,4} & b_{1,12}^{s,4} & 0 \end{bmatrix} \tag{20a}$$

first integral in the δW expression, Eq. (12a). The element applied distributed mechanical force vector $\{P\}_e$ is given by

$$\{P\}_e = \int_0^L [\zeta(\bar{x})]^T \{p(x, t)\}\, dx \quad (\{p\} = \{p_u, p_v, p_w, p_\beta\}^T) \tag{15c}$$

where $[\zeta(x)]$ is the shape function in Eqs. (13) and (14). The consistent mass matrix so obtained is a familiar one[11] and will not be given here.

The internal force vector $\{F_I\}_e$ is given by

$$\{F_I\} = [k]\{U\} + [C_v]\{\dot{U}\} + [B^a]\{V^a\} \tag{16a}$$

where $\{V^a\}$ is the piezoelastic actuator voltage vector defined by

$$\{V^a\} = \left\{ \{V^a\}_1^T \vdots \{V^a\}_2^T \vdots \cdots \vdots \{V^a\}_{n_{sa}}^T \right\}^T \tag{16b}$$

$$\{V^a\}_n = \{V^{a_n,1}, V^{a_n,2}, V^{a_n,3}, V^{a_n,4}\}^T \ (n = 1, 2, \ldots, n_{sa}) \tag{16c}$$

This internal force vector is associated with the strain energy portion in Eq. (12b) and virtual viscous damping and actuator force work terms in Eq. (12c).

Similarly the elastic stiffness matrix $[k]$ so obtained is also a familiar one[11] and will not be given here. The viscous damping matrix $[c_v]_e$ is identical to $[k]_e$ except that $\overline{EA}$, $\overline{EI_y}$, $\overline{EA_z}$, and $\overline{GJ}$ in the elements of the latter are replaced with their viscous counterparts, $\overline{\eta_E A}$, $\overline{\eta_E I_y}$, $\overline{\eta_E A_z}$, and $\overline{\eta_G J}$, respectively.

C. Actuator Force Matrix $[B^a]_e$

The actuator force vector given by the last term in Eq. (16a) is obtained from the last integral terms in Eq. (12c). With the aid of Eqs. (6a–6d) and by comparing these integral terms with Eqs. (9a–9d), it is readily shown that

$$[B^a]_e = [B^s]_{e(s\to a)}^T \tag{17}$$

That is, $[B^a]_e$ has identical form as the transpose of its sensor counterpart $[B^s]_e$ in Eq. (20a) provided that all superscripts s in the latter are replaced with superscript a (standing for actuator).

D. Sensor Voltage—Velocity Relationships

Substitution of Eqs. (13a–13d) into the strain rate sensor equations, Eqs. (9a–9d), and then the result into Eq. (10a) gives

$$\{V^s\} = -[R][B^s]\{\dot{U}\} \tag{18}$$

where $\{V^s\}$ is the sensor counterpart of $\{V^a\}$ in Eq. (16b) and $[R]$ is the $(n_{sa} \times n_{sa})$ diagonal electric resistance matrix that consisted of diagonal submatrices $[R]_n$ in Eq. (10b).

Single Sensor Layer Case with $b^{k,j} = 0$. In what follows, explicit expression for the sensor signal matrix $[B^a]_e$ and thus the actuator force matrix will be given for the single sensor actuator pair case with $b^{k,j} = 0$ in Eq. (8b). (These matrix expressions for the general case can be obtained in a similar manner.) The functions $b^{k,j}(x)$ $(j = 1\text{–}4,\ k = 1, 2)$, for example, vanish if the electrode/polarization functions $\Omega^{k,j}$ in Eq. (8c) are symmetric with respect to the y axis and z axis if $j = 1, 3$ and $j = 2, 4$, respectively; i.e.,

$$\begin{aligned} \Omega^{k,j}(x, -z) &= \Omega^{k,j}(x, z) \text{ for } j = 1, 3 \\ \Omega^{k,j}(x, -y) &= \Omega^{k,j}(x, y) \text{ for } j = 2, 4 \end{aligned} \tag{19}$$

for $k = 1$ (or s_1) (sensor layer) or $k = 2$ or a_1 (actuator layer).

Thus, for this special case,

where

$$\begin{aligned} b_{11}^{s,j} &= \bar{e}_{31}^{s,j} f_0^{s,j}/L, & b_{12}^{s,j} &= 6\bar{e}_{31}^{s,j}(2f_1^{s,j} - f_0^{s,j}L)\gamma_j^s/L^3 \\ b_{14}^{s,j} &= \bar{e}_{36}^{s,j} f_0^{s,j}\gamma_j^s/L, & b_{16}^{s,j} &= 2\gamma_j^s(3f_1^{s,j} - 2f_0^{s,j}L)\bar{e}_{31}^{s,j}/L^2 \\ & & b_{1,12}^{s,j} &= 2\gamma_j^s(3f_1^{s,j} - f_0^{s,j}L)\bar{e}_{31}^{s,j}/L^2 \end{aligned} \tag{20b}$$

for $j = 1, \ldots, 4$ with

$$\gamma_j^s = y^s \text{ if } j = 1, 3$$

$$= z^s \text{ if } j = 2, 4$$

$$f_0^{s,j} = \int_0^L a^{s,j}(x)\, dx \qquad f_1^{s,j} = \int_0^L x a^{s,j}(x)\, dx \ (j = 1, \ldots, 4) \tag{20c}$$

Consequently, in view of Eq. (17)

$$[B^a] \Rightarrow [B^{a1}] = [B^{s1}]_{(s\to a)}^T \tag{21}$$

It follows from Eqs. (11b) and (17) for the $n_p = 2$ (single case) that

$$\{V^a\} = \lceil g \rfloor [B^s]\{\dot{U}\} \tag{22a}$$

$$\lceil g \rfloor = \lceil g_A \rfloor \lceil R \rfloor \tag{22b}$$

These diagonal matrices consist of their diagonal submatrices given in Eqs. (10b) and (11b).

In view of Eq. (22a), Eq. (16a) now becomes

$$\{F_I\} = [c]\{\dot{U}\} + [k]\{U\} \quad ([c] = [c_v] + [c_p]) \tag{23a}$$

where $[c_p]$ is the piezoelectric damping matrix given by

$$[c_p] = [B^a]\lceil g \rfloor [B^s] \tag{23b}$$

V. Special Sensor/Actuator Pair Designs

A. Special Active Beam Element (Design) 1

The following conditions apply in this case.

1) Uniformly distributed surface electrode and polarization profile conditions

$$\Omega(x, y') = H(x)H(L - x)H(y' - y'^k)H(y' + y'^k) = 1$$

$$(\text{for } j = 1\text{–}4) \tag{24a}$$

for $k = s_1$ and a_1, where $H(x)$ is the Heaviside function of x.

2) Lamina angles for opposite sectors are equal in absolute values, i.e.,

$$\theta_1 = \theta_1^{k,j+2} = \pm\theta_1^{k,j} \ (j = 1, 2) \tag{24b}$$

3) The variable $\bar{d}_{3'6'} = 0$ (e.g., in the case of using PVF_2 polymer), which results in [cf. Eqs. (7b) and (7c)]

$$\bar{e}_{31}(\theta_1) = E(m_1^2 \bar{d}_{3'1'} + n_1^2 \bar{d}_{3'2'}) = \bar{e}_{31}(-\theta_1) \tag{25a}$$

$$\begin{aligned} \bar{e}_{36}(\theta_1) &= 2Gm_1n_1(\bar{d}_{3'1'} - \bar{d}_{3'2'}) \\ &= G \sin 2\theta_1(\bar{d}_{3'1'} - \bar{d}_{3'2'}) = -\bar{e}_{36}(-\theta_1) \end{aligned} \tag{25b}$$

Let $\delta_{j,j+2}^k$ $(j = 1, 2;\ k = s, a)$ be defined as

$$\delta_{j,j+2}^k = 0 \text{ if } \bar{e}_{36}^{k,j} = 0 \ (\theta_1 = 0 \text{ and/or } d_{3'1'} = d_{3'2'}) \tag{26a}$$

$$\delta^k_{j,j+2} = \bar{e}^{k,j+2}_{36}/\bar{e}^{k,j}_{36} = \sin 2\theta^{k,j+2}_1/\sin 2\theta^{k,j}_1$$
$$= 1 \text{ if } \theta^{k,j+2}_1 = \theta^{k,j}_1$$
$$= -1 \text{ if } \theta^{k,j+2}_1 = -\theta^{k,j}_1 \text{ (if } \bar{e}^{k,j}_{36} \neq 0) \quad (26b)$$

and define

$$2z^k \equiv h^k_z \text{ for } j = 1, 3; \qquad 2y^k \equiv h^k_y \text{ for } j = 2, 4 \quad (27)$$

The matrix elements b^s_{ij} in Eq. (20a) now become

$$b^{s,j}_{11} = \bar{e}^{s,j}_{31} h^s_{4-j}, \qquad b^{s,j}_{14} = \bar{e}^{s,j}_{36} h^s_y h^s_z \ (j = 1, 2)$$
$$b^{s,j}_{16} = -\bar{e}^{s,j}_{31} h^s_y h^s_z/2, \qquad b^{s,j}_{1,12} = \bar{e}^{s,j}_{31} h^s_y h^s_z/2 \ (j = 1, 2) \quad (28)$$
$$b^{s,j}_{12} = 0 \ (j = 1, 2) \ (h^s_2 \equiv h^s_y, \ h^s_3 \equiv h^s_z)$$

The corresponding piezoelectric dumping matrix $[c_p]$, after carrying out the matrix multiplications in Eq. (23b) by using Eqs. (20a), (21), and (29), is obtained as

$$[c_p] = \begin{bmatrix}
p_{NN} & 0 & 0 & -p_{N\beta} & 0 & 0 & -p_{NN} & 0 & 0 & p_{N\beta} & 0 & 0 \\
0 & 0 & 0 & 0 & 0 & 0 & 0 & 0 & 0 & 0 & 0 & 0 \\
0 & 0 & 0 & 0 & 0 & 0 & 0 & 0 & 0 & 0 & 0 & 0 \\
-p_{\beta N} & 0 & 0 & p_{\beta\beta} & -p_{\beta y} & p_{\beta z} & p_{\beta N} & 0 & 0 & -p_{\beta\beta} & p_{\beta y} & -p_{\beta z} \\
0 & 0 & 0 & -p_{y\beta} & p_{yy} & 0 & 0 & 0 & 0 & p_{y\beta} & -p_{yy} & 0 \\
0 & 0 & 0 & p_{z\beta} & 0 & -p_{zz} & 0 & 0 & 0 & -p_{z\beta} & 0 & -p_{zz} \\
-p_{NN} & 0 & 0 & p_{N\beta} & 0 & 0 & p_{NN} & 0 & 0 & -p_{N\beta} & 0 & 0 \\
0 & 0 & 0 & 0 & 0 & 0 & 0 & 0 & 0 & 0 & 0 & 0 \\
0 & 0 & 0 & 0 & 0 & 0 & 0 & 0 & 0 & 0 & 0 & 0 \\
p_{\beta N} & 0 & 0 & -p_{\beta\beta} & p_{\beta y} & -p_{\beta z} & -p_{\beta N} & 0 & 0 & p_{\beta\beta} & -p_{\beta y} & p_{\beta z} \\
0 & 0 & 0 & p_{y\beta} & -p_{yy} & 0 & 0 & 0 & 0 & -p_{y\beta} & p_{yy} & 0 \\
0 & 0 & 0 & -p_{z\beta} & 0 & -p_{zz} & 0 & 0 & 0 & p_{z\beta} & 0 & p_{zz}
\end{bmatrix} \quad (29a)$$

where

$$p_{NN} = 2(g_1 h^a_z h^s_z \bar{e}^{a,1}_{31} \bar{e}^{s,1}_{31} + g_2 h^a_y h^s_y \bar{e}^{a,2}_{31} \bar{e}^{s,2}_{31})$$
$$p_{N\beta} = h^s_y h^s_z [g_1 h^a_z \bar{e}^{a,1}_{31} \bar{e}^{s,1}_{36}(1 + \delta^s_{13})/2 + g_2 h^a_y \bar{e}^{a,2}_{31} \bar{e}^{s,2}_{36}(1 + \delta^s_{24})/2]$$
$$p_{\beta N} = h^a_y h^a_z [g_1 h^s_z \bar{e}^{s,1}_{31} \bar{e}^{a,1}_{36}(1 + \delta^a_{13})/2 + g_2 h^s_y \bar{e}^{s,2}_{31} \bar{e}^{a,2}_{36}(1 + \delta^a_{24})/2]$$
$$p_{\beta\beta} = h^4 [g_1 \bar{e}^{a,1}_{36} \bar{e}^{s,1}_{36}(1 + \delta^s_{13}\delta^a_{13})/2 + g_2 \bar{e}^{a,2}_{36} \bar{e}^{s,2}_{36}(1 + \delta^s_{24}\delta^a_{24})/2]$$
$$p_{\beta y} = h^4 g_2 \bar{e}^{a,2}_{36} \bar{e}^{s,2}_{31}(1 - \delta^a_{24})/4$$
$$p_{\beta z} = h^4 g_1 \bar{e}^{a,1}_{36} \bar{e}^{s,1}_{31}(1 - \delta^a_{13})/4 \quad (29b)$$
$$p_{y\beta} = h^4 g_2 \bar{e}^{a,2}_{31} \bar{e}^{s,2}_{36}(1 - \delta^s_{24})/4 \qquad (h^4 \equiv h^a_y h^a_z h^s_y h^s_z)$$
$$p_{yy} = h^4 g_2 \bar{e}^{a,2}_{31} \bar{e}^{s,2}_{31}/2$$
$$p_{z\beta} = h^4 g_1 \bar{e}^{a,1}_{31} \bar{e}^{s,1}_{36}(1 - \delta^a_{13})/4$$
$$p_{zz} = h^4 g_1 \bar{e}^{a,1}_{31} \bar{e}^{s,1}_{31}/2$$

with

$$g_3 = g_1 = g^{1,1}_A R^{1,1}_A, \qquad g_4 = g_2 = g^{1,2}_A R^{1,2} \quad (29c)$$

In arriving at Eqs. (29a) and (29b), it was assumed that $g_3 = g_1$ and $g_4 = g_2$, where the various g are the diagonal elements of the diagonal matrix $[g]$ in Eq. (22b). In view of Eqs. (10a) and (11a), these parameters are given by Eq. (29c). The thicknesses of two adjacent piezoelastic layers are negligibly thin compared with beam depth and width. Because of this, the piezoelectric damping matrix $[c_p]$ can be regarded as symmetric, although no such matrix property is actually used in arriving at Eq. (29a).

B. Special Active Beam Element (Design) 2 (No Cross Coupling Effect Case)

The matrix expressions in Eqs. (29a) and (29b) show that the coupling among piezoelastically induced bending/torsion/axial force components can be decoupled if the four sensor/actuator pairs at the four sectors (sides) of the rectangular cross section are properly designed in the following way:

1) Use the same piezoelectrical materials with $d_{3'6'} = 0$ (such as PVF_2 material) for both sensor and actuator layers.

2) Make piezoelectric lamina angles to be (Fig. 4)

$$\theta^{k,1}_1 = \theta^{k,3}_1 = -\theta^{k,2}_1 = -\theta^{k,4}_1 \equiv \theta \qquad (k = s, a) \quad (30a)$$

3) Design $R^{s,1}g_1$ and $R^{s,2}g_2$ such that

$$g_2/g_1 = h^a_z/h^a_y \cong h^s_z/h^s_y \quad (30b)$$

4) The conditions in Eq. (30b) are satisfied if

$$t^k_z \ll h^k_z, \qquad t^k_y \ll h^k_y \text{ so that } h^s_i \cong h^a_i \ (i = y, z)$$

The first and second conditions result in

$$\delta^k_{13} = \delta^k_{24} = 1 \text{ if } \sin 2\theta \neq 0 \ (k = s, a) \quad (30c)$$
$$\bar{e}^{a,j+2}_{31} = \bar{e}^{s,j}_{31} = \bar{e}^{s,j+2}_{31} \equiv \bar{e}_{31} \ (j = 1, 2) \quad (30d)$$
$$\bar{e}^{k,2}_{36} = -e^{k,1}_{36} \equiv \bar{e}_{36} \ (k = s, a) \quad (30e)$$

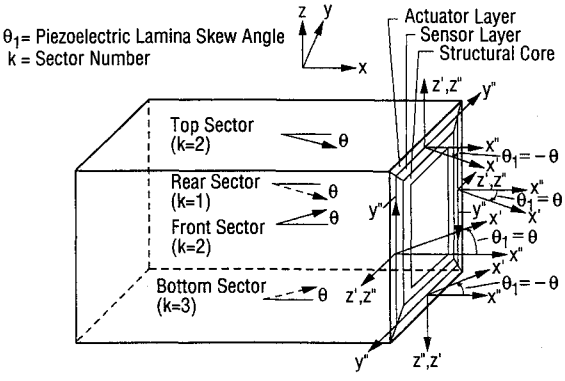

Fig. 4 Lamina skew angle relationship among four-sectored sensor/actuator pairs for special no. 2 beam element design.

Also, from conditions in Eqs. (30b–30e), all cross-coupling terms vanish, and Eqs. (29b) reduce to

$$p_{N\beta} = p_{\beta N} = p_{\beta y} = p_{y\beta} = p_{z\beta} = p_{\beta z} = 0$$

$$p_{NN} = 2gh_z^a(\bar{e}_{31})^2(h_y^a + h_y^a)$$

$$p_{BB} = g\bar{h}_z^2 h_y^s(\bar{e}_{36})^2(\bar{h}_y^a + h_z^a)/2 \qquad (31a)$$

$$p_{yy} = gh_y^a\bar{h}_z^3(\bar{e}_{31})^2/2$$

$$p_{zz} = g(\bar{h}_y)^2(\bar{h}_z)^2(\bar{e}_{31})^2/2$$

where

$$\bar{h}_1 = (h_1^s + h_1^a)/2; \qquad i = y, z$$

$$g \equiv g_1 = V^{a,1}/i^{s,1} = g_A^{a1,1}R^{s1,1} \qquad (31b)$$

VI. Application of Active Beam Elements in Vibration Control/Analysis of a Space Antenna Frame Structure

In this section, the specially designed no. 2 active piezoelectric beam elements whose force-deformation relationships are free from cross- coupling effects are used as the active beam elements in vibration control/transient response analysis of an example adaptive space antenna frame structure.

A. Computer Code for Transient Response Analysis of Adaptive Space Frame Structures

The element force-displacement relationships for the newly developed multiaxially active beam elements are given by Eqs. (14) and (23) with the piezoelectric damping matrix $[c_v]$ given by Eqs. (23b) for the general design case and Eqs. (29a–29c) and Eqs. (29a) and (31a) for the special design 1 and 2 cases, respectively. The finite element method based, computerized transient response analysis procedure for the adaptive frame structures composed of regular (passive) and the newly developed active beam elements is essentially the same as its non-adaptive structure counterpart provided that an additional piezoelectric damping force term is present in the equations of motion.

In the present study, the finite element model of the special active beam element design 2 has been implemented in the previously developed massively parallel, prototype CM-2 computer code, CM-DYNASTAN, as well as on a serial Sparc-2 SUN workstation as a SUN-DYNAN code. As a result, CM-DYNASTAN is capable of superefficiently performing the static and dynamic response analyses of three-dimensional regular and adaptive frame/truss structures as well as static structural optimization in the massively parallel environment of the CM-2 computer.[12]

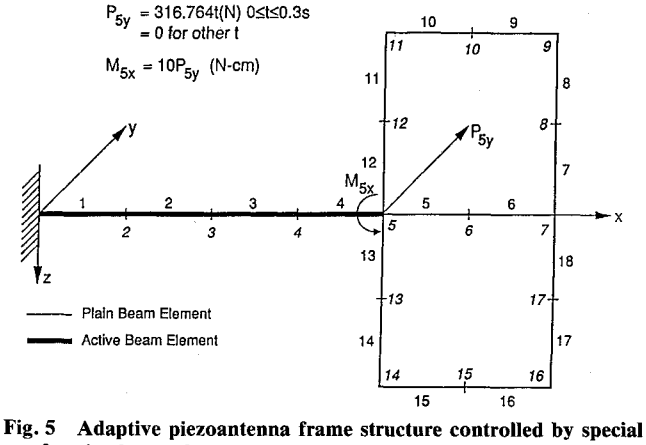

Fig. 5 Adaptive piezoantenna frame structure controlled by special no. 2 active beam elements.

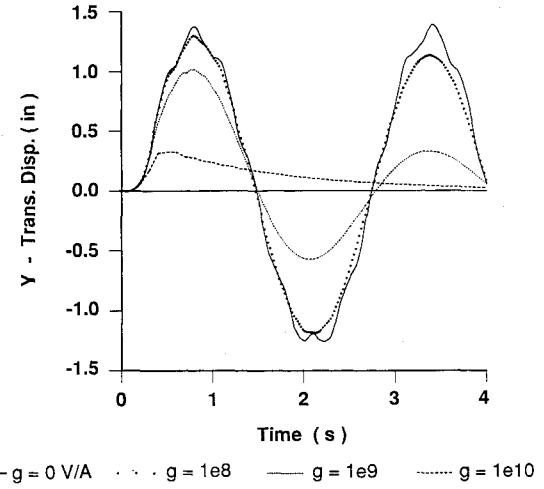

Fig. 6 y-translational displacement responses for nodal point 9 of piezoantenna under various values of current gain g (V/A).

B. Example Transient Piezo Antenna Frame Response Analysis Problem

1. Description of the Example Problem

Figure 5 shows an active beam deployment configuration of an 18-finite-beam element model of a space antenna structure subjected to a y-transverse force, P_{5y}, and x-axis torsional moment, M_{5x}, at nodal point 5. This structure, with all regular (nonactive) beam elements and concentrated controllers and using the basic eight-member model with seven nodal points at joints, was used as an example problem elsewhere[13] for an optimal placement study of concentrated actuators/sensors. The regular beam elements 1–4 are replaced here by active beam elements to control structural vibrations. All cross sections of regular and active beam elements are assumed to be of the hollow square type with a depth (width) of 20 cm and a wall thickness of 0.5 cm. All regular beams and host structure portions of active beam elements are fabricated from aluminum material with $E = 10.3 \times 10^6$ psi, $G = 4.5e + 6$ psi, and mass density $= 2.4093 \times 10^{-4}$ lb-s^2/in. The four sensor/actuator pairs, one pair each bonded to the four outer surfaces of each active beam element, are assumed to be fabricated from piezoelectric PVF_2 films with sensor and actuator layers each having thickness of 0.022 cm (i.e., the double thickness) and the trade name KYNAM™. For the latter, $E_p = 2 \times 10^9$ N/M^2, $\rho_p = 1780$ kg/m^3, ν_p (Poisson's ratio) $= \frac{1}{3}$, $d_{3'1'} = 23 \times 10^{-12}$ m/V, and $d_{3'2'} = 3 \times 10^{-12}$ m/V. For the present example problem, the skew angles θ_1 of all piezoelectric laminae are assumed to be 45 deg.

In what follows, mechanical (viscous) damping forces are omitted because the main interest here is in studying and understanding the effect of piezoelectric damping on transient structural response behavior.

2. Transient Response Analysis Results

Figures 6–8 show the y-translational and x- and z-rotational transient displacement responses of nodal point 9 of piezoantenna for the open-loop ($g = 0$) and closed-loop ($g > 0$) cases for various values of g; the gain of the current amplifier is given by Eq. (31b) with units of volt/ampere. The x- and z-rotational displacement components are mainly associated with the first torsional and bending vibration modes of the entire structure, respectively, although significantly higher mode effects are also present for the undamped ($g = 0$) or nonsignificantly damped cases. In the closed-loop case, no appreciable piezoelectric damping effect is observed until g reaches the level of $1.e + 7$ V/A as can be seen from Figs. 7 and 8. At $g = 1.e + 8$ V/A, the higher mode portions of vibration are entirely suppressed as can be seen clearly from Figs. 8a and 8b. At $g = 1.e + 9$ V/A, significant attenuations of the major (lower or lowest mode) portions of vibration are

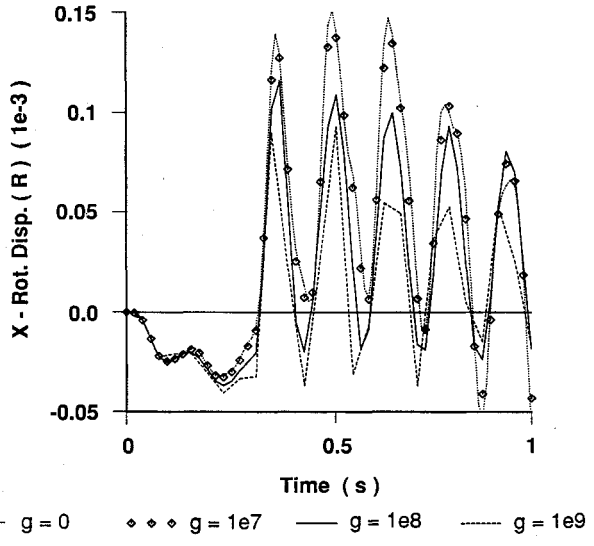

Fig. 7a *x*-rotational displacement responses for nodal point 9 of piezoantenna under various values of g (V/A) for t = 0–1 s case.

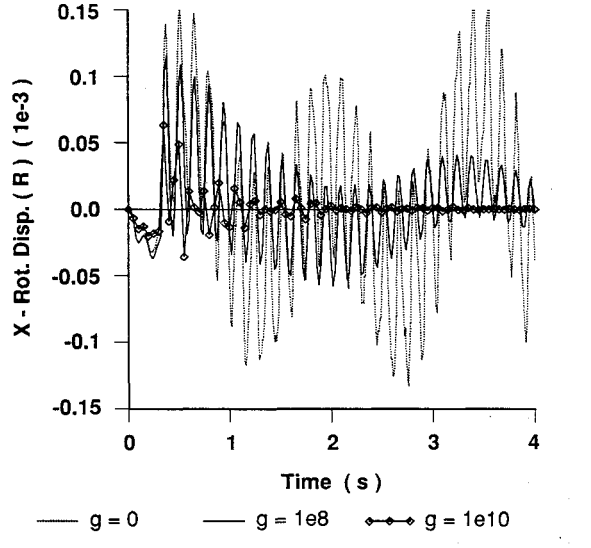

Fig. 7b *x*-rotational displacement responses for nodal point 9 of piezoantenna under various values of g (V/A) for t = 0–4 s case.

seen. Finally, at the $g = 1.e + 10$ V/A level, overdamped vibration behavior is seen for both y-translational and z-rotational bending response cases (Figs. 6 and 8), whereas near-critical vibration behavior is seen for the x-rotational response case. In this case, completion of vibration suppressions are accomplished within two undamped free vibration periods for the y-translational and z-rotational displacement response cases and a few quick cycles of vibrations for the x-rotational displacement response case.

It should be noted that the analytical predictive techniques based on the present linear theory are valid as long as the piezoelectric material behaves linearly under mechanical and/or electrical loadings. Also the increase of current amplifier gain level to increase vibration control efficiency is achievable as long as the piezoelectric material does not fail under a high-voltage condition. An analysis of voltage data showed that the 0.022-cm-thick piezoelectric actuator films can maintain their integrity for a g-value of $1e + 7$ V/A at the most. Therefore, to provide enough control authority (equivalent to a g-level of $1e + 9$ to $1e + 10$ V/A) for effective vibration suppression of the space antenna structural subsystem studied, most (if not all) of the following additional measures are needed: 1) increase in piezoelectric layer thicknesses; 2) use of more authoritative piezoelectric material, such as the PZT

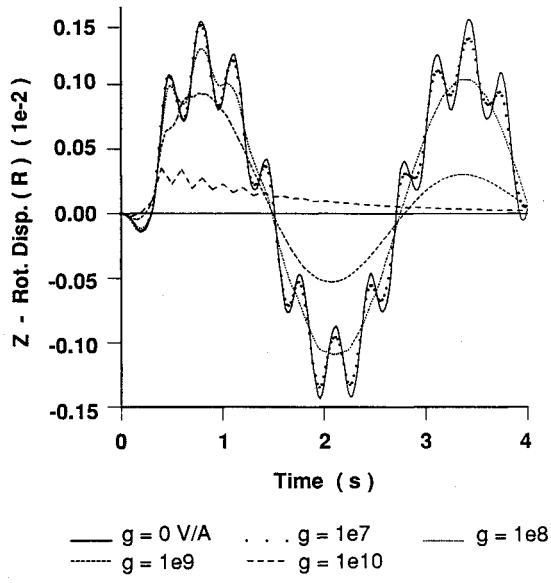

Fig. 8 *z*-rotational displacement responses for nodal point 9 of piezoantenna under various values of g (V/A).

ceramic one; 3) use of optimized nonuniform surface electrode pattern and/or polarization profile; and 4) deployment of optimal number and locations of active beam elements.

VII. Conclusions

Development of a general finite element model for multiaxially active, laminated piezoelectric beam sensor/actuator element has been made. It was then used in the design of two detailed active beam sensor/actuator pair elements and the development of associated special finite element models under the uniform surface electrode distribution/polarization profile condition and certain skew angle relationships among various sector's laminae. The structural vibration control efficiency of such multiaxially active beam sensor/actuator elements was demonstrated here through a numerical transient response problem of an adaptive piezoelectric space antenna structure composed of regular (passive) beam and the special active beam elements, negative strain rate feedback control design type developed herein. From these numerical transient response study results, it can be concluded that the four-sectored piezoelectric sensor/actuator design is not only feasible but also efficient in simultaneously controlling all three-dimensional vibration components via complete control of all deformation components (axial extension, biaxial bending, and twisting deformations) of the active beam elements. Although the mathematical model developed herein is a linear and elementary one, it retains all the key fundamental parameters/features needed to explore/design integrated piezoelectric sensors/actuators. However, much more work must be done to bring the research results to full fruition. Further efforts must be made in the follow-on study in the following areas. The developed piezoelectric beam sensor/actuator designs should be refined by, say, using nonuniform polarization profiles and/or surface electrode patterns. The experimental verifications of the piezoelectric beam sensor/actuator designs and the analytical predictive models and techniques developed must be performed. The study of the parametric optimization of the piezoelectric sensor/actuator design case must be extended, as well as the development of optimal active beam placement techniques and the extension of the numerical vibration control efficiency evaluation study to other piezoelectric materials, such as the piezoceramic (PZT) material. Also desirable is an extension of the theory to include inherent piezoelectric material and time-dependent nonlinearities (which are particularly important in sensor/actuator integrity analysis), shear deformation and rotatory inertia effects (which are particularly important for the short beam case with

wavelength/beam depth ratio <5 and/or advanced composite host structure cases), etc.

Acknowledgments

This work, except for most of Sec. VI, was supported by Strategic Defense Initiative/Innovation Science and Technology and managed by United States Air Force Phillips Laboratory under Contract F29601-91-C-0062.

References

[1]Shieh, R. C., "Multiaxial Piezoelectric Beam Sensors/Actuators Theory and Design for 3-D Structural Vibration Control," *Proceedings of Third International Conference on Adaptive Structures* (San Diego, CA), Nov. 9–11, 1992, pp. 647–661.

[2]Shieh, R. C., "Massively Parallel Computational Control/Structure Interaction Dynamics Including Development of Multiaxial Laminated Piezoelectric Beam Sensor/Actuator Elements," Strategic Defense Initiative Organization Contract F29601-91-C-0062, Final Rept., April 1992.

[3]Hanagud, S., Obal, M. W., and Claise, A. J., "Optimal Vibration Control by the Use of Piezoceramic Sensors and Actuators," *Proceedings of the AIAA/ASME/ASCE/AHS/ASC 28th Structures, Structural Dynamics, and Materials Conference,* AIAA, Washington, DC, 1987, pp. 987–997 (AIAA Paper 87-0959).

[4]Crawley, E. F., and de Luis, J., "Use of Piezoelectric Actuators as Elements of Intelligent Structures," *AIAA Journal,* Vol. 25, No. 10, 1987, pp. 1373–1385.

[5]Baily, T., and Hubbard, J., "Distributed Piezoelectric Polymer Active Vibration Control of Cantilever Beam," *Journal of Guidance, Control, and Dynamics,* Vol. 8, No. 5, 1987, pp. 605–611.

[6]Hagwood, N. W., Chung, W. H., and von Flotow, A., "Modeling of Piezoelectric Actuator Dynamics for Active Structural Control," *Proceedings of the AIAA/ASME/ASCE/AHS/ASC 31st Structures, Structural Dynamics, and Materials Conference* (Long Beach, CA), AIAA, Washington, DC, 1990, pp. 2242–2256 (AIAA Paper 90-1087).

[7]Cudney, H., Inman, D. J., and Oshman, Y., "Distributed Structural Control Using Multilayered Piezoelectric Actuators," *Proceedings of the AIAA/ASME/ASCE/AHS/ASC 31st Structures, Structural Dynamics, and Materials Conference* (Long Beach, CA), AIAA, Washington, DC, 1990, pp. 2257–2264 (AIAA Paper 90-1088).

[8]Lee, C.-K., "Piezoelectric Laminates for Torsional and Bending Modal Control: Theory and Experiment," Ph.D Thesis, Cornell Univ., Ithaca, NY, 1987.

[9]Lee, C.-K., "Piezoelectric Laminates: Theory and Experiments for Distributed Sensors and Actuators," *Intelligent Structural Systems,* edited by H. S. Tzou and G. L. Anderson, Kluwer Academic Publishers, Boston, MA, 1992, pp. 75–167.

[10]Boley, B. A., and Weiner, J. H., *Theory of Thermal Stresses,* Wiley, New York, 1960, Chap. 14.

[11]Przemieniecki, J. S., *Theory of Matrix Structural Analysis,* McGraw-Hill, New York, 1968.

[12]Shieh, R.C., "Massively Parallel Computational Methods for Finite Element Analysis of Transient Structural Responses," *Proceedings of the 2nd Symposium on Parallel Computational Methods for Structural Analysis and Design* (Norfolk, VA), Feb. 24–25, 1993; also *Journal of Computing Systems in Engineering* (to be published).

[13]Sepulveda, A. E., and Schmidt, L. A., Jr., "Optimal Placement of Actuators and Sensors in Control Augmented Structural Optimization," *Proceedings of the AIAA/ASME/ASCE/AHS/ASC 32nd Structures, Structural Dynamics, and Materials Conference,* AIAA, Washington, DC, 1990, pp. 217–240 (AIAA Paper 90-1055).

[14]Timoshenko, S. P., "On the Correction for Shear of the Differential Equation for Vibration of Prismatic Bars," *Phylosophy Magazine,* Vol. 41, 1921, pp. 744–746.

[15]Song, O., Librescu, L., and Rogers, C. A., "Application of Adaptive Technology to Static Aeroelastic Control of Wing Structures," *AIAA Journal,* Vol. 30, No. 12, 1992, pp. 2882–2889.